Real Time Strain Imaging – a new Ultrasonic Method for Cancer Detection: First Study Results

A. Pesavento, A. Lorenz

Lorenz & Pesavento IT, Ehrenfeldstr 34, 44789 Bochum

E-Mail Adresse: lp@lp-it.de

ABSTRACT

Prostate tumors can have a higher mechanical hardness than the surrounding tissue. During the digital rectal exam this can be used not only to detect the hypertrophy but also localized hardenings. The examination by digital palpation is inaccurate and even in combination with PSA-value and a transrectal ultrasonic examination the result is often not reliable. Ultrasound strain imaging is able to measure and visualize the elastic properties of a tissue region and hence is an adequate supplement for commonly used diagnostic procedures.

We have developed a real time system for elastographic mechanical tissue assessment of the prostate which can be used for the transrectal ultrasonic examination for navigation and diagnosis. During the examination a sequence of ultrasonic images is acquired while the organ is slightly compressed by the ultrasound probe. Using a numerical analysis of image pairs of the acquired sequence the tissue strain is calculated which represents the spatial elasticity distribution of a specific cross-section of the organ and which are able to distinguish hard areas in the tissue.

We present results from several patients. which show, that real time strain imaging is able to detect tumor-like areas which are inconspicuous in the b-mode image. The results correspond to the histological specimens. After the evaluation of 130 patients using a prospective study we found the specificity for cancer detection to be approximately 84% and a sensitivity of approximately 76 %. Furthermore the tumor location and extend was correctly predicted in most of the investigated patients using our real time strain imaging.

SIGNAL PROCESSING

Strain imaging was first described by Ophir in 1991 [1], but could not easily be clinically applied so far, because the described method had no real time capability. To use it in a clinical setting we invented a time efficient algorithm, called "phase root seeking" [2], which in a current system is able to calculate up to 30 strain images per second using a conventional desktop PC. Similar to [1], time shifts are estimated using a discrete number of windows at discrete depths. The time shift $\tau_{m,k}$ of the k-th window of two A-lines centered around $t_k = k\Delta T$ is estimated by the following iterative formula

$$\tau_{m,k,0} = \tau_{m,k-1,L} \tag{1}$$

$$\tau_{m,k,l} = \tau_{m,k,l-1} +$$

$$\frac{1}{\omega_0} \arg\left(e^{-j\omega_0 \tau_{m,k,l-1}} \int_{t_k-T_w/2}^{t_k+T_w/2} b_1^*(t) b_2(t - \tau_{m,k,l-1}) dt \right)$$

where $b_1(t)$ and $b_2(t)$ denote the corresponding precompression and postcompression baseband echo data, and l is an iteration index. $L = 2$ iterations are used in our systems. The quantity ω_0 denotes the transducers nominal center frequency. T_w denotes the window length. Aliasing of the arg-function can be successfully avoided, if the difference of the time delays of two successive windows is smaller than π/ω_0, which is usually valid for small transducer motion. When phase root seeking is applied to digital signals the integral is replaced by a sum. Furthermore, the postcompression signal has to be time-shifted by a sub-sample time shift [3]. This is done using linear interpolation of baseband signals. Hence sub-
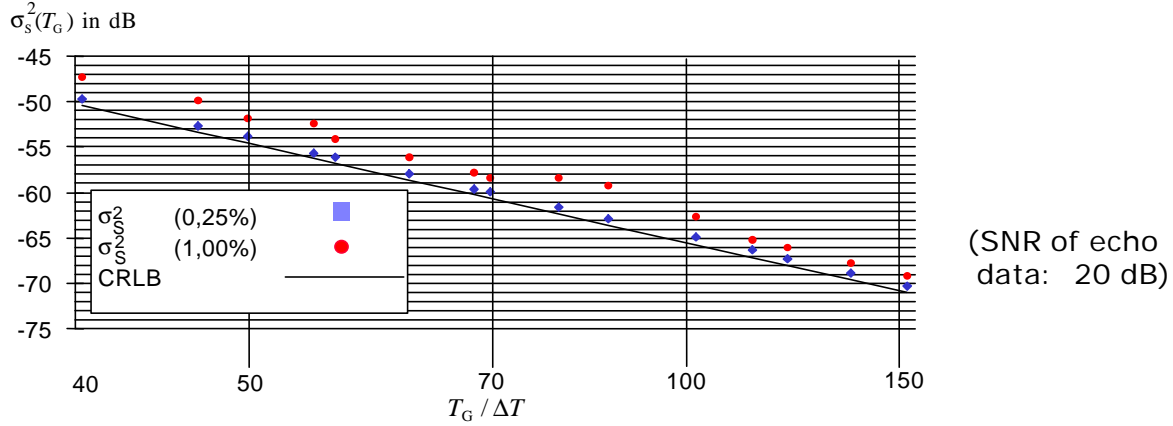
Figure 1: Comparison of strain variance to its Cramer Rao Lower Bound as a function of observation length T_G for two different strains

sample time-shifts can be estimated. Linear interpolation is more accurate for baseband data, this is the reason why phase root seeking uses baseband data instead of complex rf echoes (analytic signals).

Strain is estimated from time delays by a generalized least square estimator [4]

$$\begin{pmatrix} \hat{s} \\ \hat{t}_0 \end{pmatrix} = (A^T W^{-1} A)^{-1} A^T W^{-1} \vec{\tau} \qquad (2)$$

In this estimator, the slope $\hat{s}$ of the time delays $\vec{\tau}$ is estimated using a least square fit that takes into account correlations of estimated time delays, described by a covariance matrix W. Time delays are correlated since they are estimated using overlapping windows. Matrix A describes the linear relationship between time delay and strain. Using simulations, in [2] we compared the strain variance to its corresponding Cramer Rao Lower Bound [5]:

$$\sigma_s^2 \geq \frac{24\pi}{T_G^3} \left(\int_0^\infty \frac{2\omega^2 C_{UU}^2(\omega) / C_{nn}^2(\omega)}{1 + 2C_{UU}(\omega) / C_{nn}(\omega)} d\omega \right)^{-1} \qquad (3)$$

In this expression $C_{UU}(\omega)$ denotes the power spectrum of the echo signals , $C_{nn}(\omega)$ denotes the noise spectrum and T_G the observation time. These Simulations have shown, that for small strains of approximately 0.25 %, strain estimation is nearly ideal (Fig. 1). Note, however, that these simulation do not take into account motion artefacts.

If these low strains (<0.25%) are used, the signal-to-noise ratio (SNR) of strain images can be

increased by multicompression approaches [11]. In a real time strain imaging system the summation of successive rf-frames can be described by temporal filtering of strain images using a filter with rectangular impulse response (note that temporal filtering means a filtering of successive frames on the "slow" time axis and not axial filtering of one image). Such a filter is not ideal in this situation, because the user of the system experiences a time-lag between the application of a tissue compression an the visual reaction of the system, which is an increasing strain on the screen. This effect is less severe, if a recursive filter of the form

$$\bar{s}_m = s_m + p\bar{s}_{m-1}$$

is used, where s_m denotes the m-th strain image. The filtering effect and the noise reduction of this filter is similar to the filter with the rectangular impulse response. Temporal filtering of strain images is described in detail in [7]

When choosing the frame rate in a real-time system, the main question for the data acquisition is the following: is it better to use high-frame rate data acquisition, resulting in many low SNR strain images per second, which can be used for further filtering, or is it better to use lower frame rates, resulting in less but higher SNR strain images per second and perform no or less temporal filtering of strain images. Fig. 2 illustrates this question: using a given amount of strain (given either by physiological reasons or being an amount of compression, that can reasonably be applied in a fixed time), the question has to be answered whether it is better to acquire several e.g. 5 rf-frames during this compression and form the resulting strain images using a summation of these

strain images (4 in this example) or is it better to calculate one strain image using only the first comparing to the last rf-frame?

To answer this question, we have to look separately into the two different kinds of noise
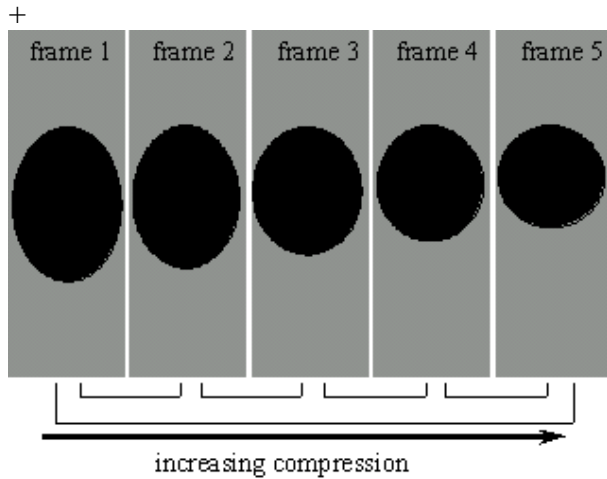
Figure 2: Strain images can be estimated by comparing frame 1 and frame 5 or by summing up the four strain images obtained by comparing successive frames.

observed on strain images. First considering only decorrelation noise, which results from undesired tissue motion or speckle decorrelation, the answer is obvious: since the amount of this noise is proportional to the amount of applied strain (for higher strains the dependency is even of a higher order), it is favorable to divide the compression in as many high correlated frames as possible.

Another component of noise in strain images results from the noise of the rf-echoes. When looking at the Cramer-Rao-Lower Bound for strain estimation in Equation 3 we see, that this noise is totally independent from the applied strain.

In order to find out, which of the to options outlined in Fig. 2 is preferable with respect to noise performance, in [6] we analyzed correlation of the strain in single images using simulation. Using the results, we showed that, when looking at noise resulting from imperfect rf-data (electronic and acoustic noise etc.) one may use any number of steps during the tissue compression and combine the resulting strain images to one strain image. The strain image may as well be estimated using a single big compression step, this will result in the same SNR. This result is interesting, because it shows, that the use of high frame rates do not deteriorate the SNR of the strain images. However, when looking at decorrelation noise, which is a major problem especially in in vivo situations, we decrease this kind of noise by increasing the

correlation of the rf-frames due to an increase of the number of acquired rf-frames which decreases the compression between two frames.

SYSTEMS

Our experience using an offline approach described in [8] was also used for the implementation the current systems. Currently we use two system for clinical evaluation:

The first system operates with a 7.5 MHz transrectal probe connected to a Combison 330 scanner from Kretztechnik AG/Austria. The rf-data are directly sampled into the PC-memory by a PC-card (GaGe™) with a sampling frequency of 25 MHz and 12 bit resolution. Using the transrectal probe 20 frames per second are acquired and processed. Within a region of interest of approximately 2.5 cm x 3.6 cm the real time strain images are calculated and displayed. The rf-data of two successive frames in the PC-memory are used as pre- and post-compression images. The absolute value of the strain is displayed color-coded on the PC monitor side by side with the b-mode image including a real time scan conversion of the b-mode image and the strain image. The strain is evoked by compressing and releasing the tissue with the hand held transducer itself. For the calculation and the display a Dual Pentium™ 800 MHz Desktop PC with 384 MB RAM is used. A strain image has the approximate size of 100 x 90 pixels. The rf-data are acquired and evaluated continuously in real time.

The second system uses a Kretz Voluson V730 for both, the data acquisition and strain estimation. Strain images are displayed next to the b-mode image on the systems screen.

PHANTOM IMAGES

To demonstrate typical images of the system, a phantom has been constructed which consists of a sponge in which hard lesions have been included by injecting a 3 % agar-agar solution. The hard lesion is about 10 times stiffer than the surrounding sponge. Fig. 3 shows typical strain images obtained using the static strain imaging concept with manual application of the compression using a hand-held transducer. The strain is displayed by grayscale map. Bright regions denote high strains, dark regions low strain. The images shows the typical strain patterns around a hard lesion, simulated by FEM methods by many authors e. g. [10] The low SNR in the lower right and lower left
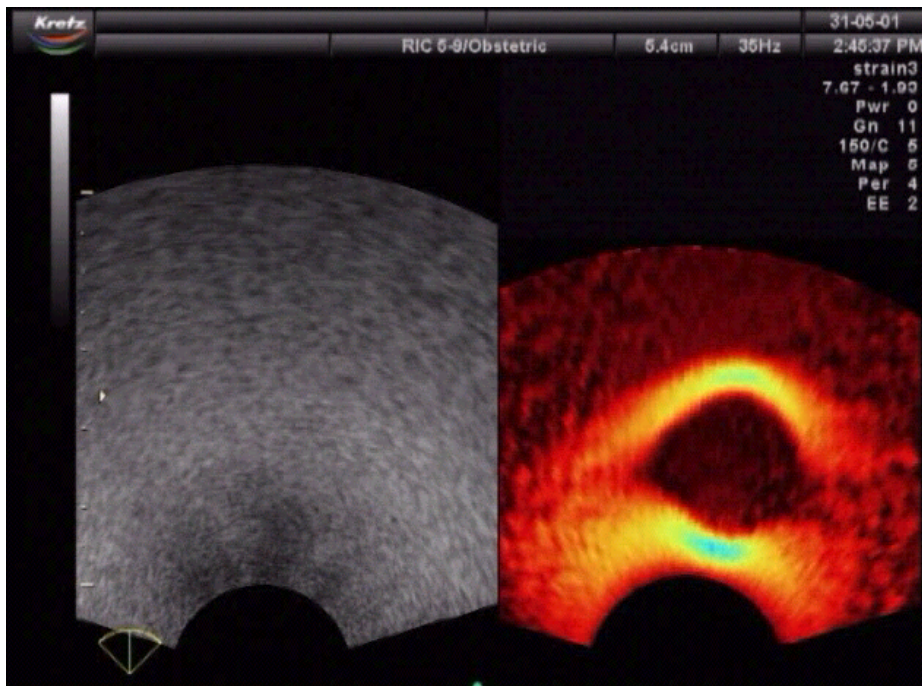
Figure 3: left: b-mode image, middle: strain image of a phantom with a hard inclusion produced by the injection of agar agar

region of the image are due to decorrelation noise caused by the use of a sector probe [11]

CLINCIAL TRIAL

Currently the method is evaluated in a clinical trial the Marienhospital in Herne, University Hospital of the Ruhr-University of Bochum. All patients were examined using the same clinical procedure. First, the conventional examination was done which included determination of the PSA value, digital palpation, conventional ultrasound. If necessary, a biopsy was taken to obtain a conventional diagnosis. In addition all patients with positive biopsies who had to undergo radical prostatectomy were examined with real time strain imaging prior to their operation. Real time strain imaging was used to determine the location and the size of the tumor in one of six quadrants, i.e. on the right and left side in the apical, middle and base part of the prostate. In most of the cases the tumor could not be detected with conventional ultrasound at all. Some of the patients had an irregular unsymmetrical shape of the gland using conventional B-mode imaging. After the radical prostatectomy the prostate was processed by a pathologist and three full size histological cross-sections were obtained from the apical, middle and base part of the gland. A microscope was used to determine and mark the exact location and extend of the tumor in the three cross-sections. The histology was photographed and compared to the strain images.

RESULTS

In this section we will present an example for an in vivo real time strain image which shows that real time strain imaging is able to detect hard tissue regions which correspond to tumor locations in the histological cross-sections.

The histologies in Figure 4 (right) shows, that the tumor is located on the right hand side of the image close to the transducer. It can be clearly identified in the strain image by a dark red area, but it can hardly be seen in the b-mode image. Note, that the boundary of the prostate is well defined by a high strain border (bright) which is due to the soft fatty layer which surrounds the gland. In the upper b-mode image there are two stones in the center of the gland which can be recognized in the strain image as dark red spots.

So far we have analyzed the data of 130 patients. Using this data for this method a specificity of 84% and a sensitivity of 76% was found. To get a true positive result we decided 50% of the cancerous area had to be detected at an exact
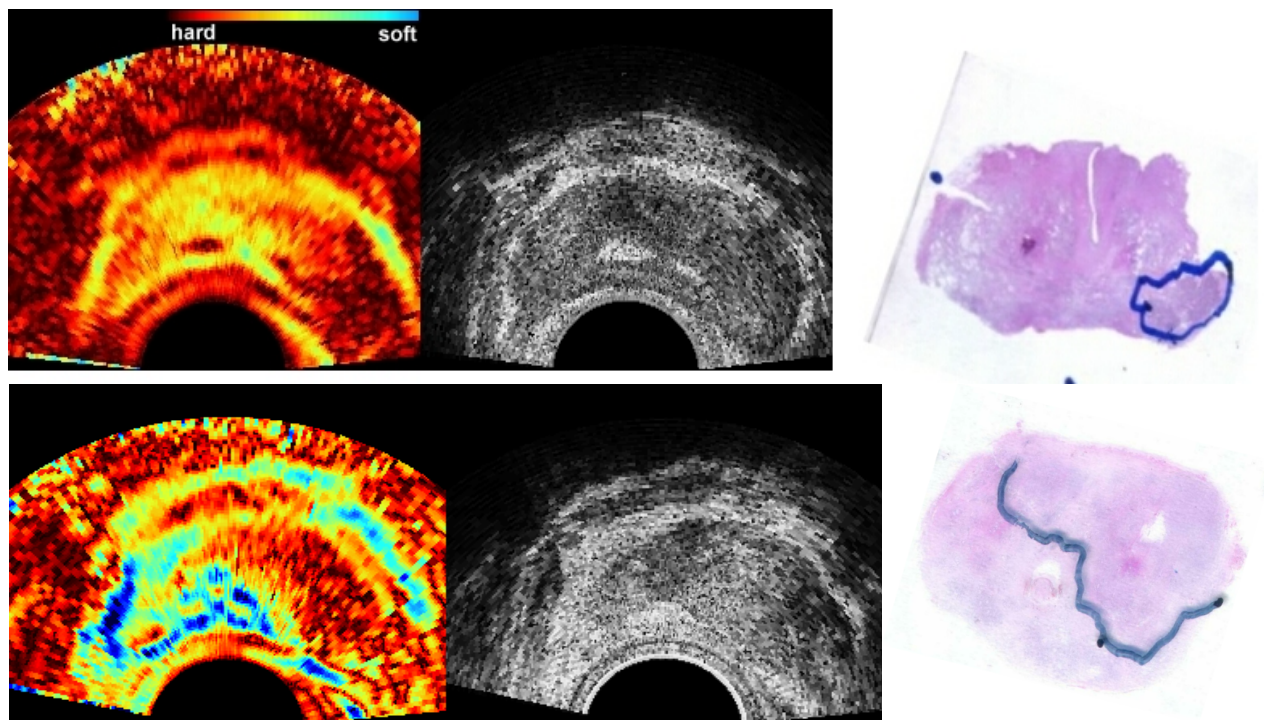
Figure 4: left = strain images, middle = b-mode images, right = histology images with marked tumor regions. The histologies shows, that both tumors are located on the right hand side of the image. It can be clearly identified in the strain image, but hardly be seen in the b-mode image.

position using the histology as the "gold standard" method.

Note, that this study is conducted prospectively, i.e. the examiner must define the tumor dimension and location directly after the ultrasonic real time strain examination at a point where no histological specimen is available.

CONCLUSIONS

In this paper we presented the development of a new systems for real time strain imaging based on a conventional PCs connected to a conventional ultrasound machine. The systems were used for in vivo real time examinations of the mechanical properties of prostate tissue with the aim to improve conventional ultrasonic diagnosis of prostate carcinoma. Prostate carcinoma is most often not recognizable by the b-mode image [9], but can often be detected by a combination of digital palpation and PSA value. So far ultrasonic imaging was found not to yield valuable information about cancer position and dimension. However, the findings described above show that very often hardenings can be localized by strain imaging and estimated in their true dimensions where b-mode imaging can not.

We implemented the world's first real time strain imaging system. We used a conventional PC

platform which allows easily scaling of speed and memory with improving PC technology. At the moment our system is able to calculate and display up to 30 images per second with approximately 10000 pixels each. The resulting real time strain images are displayed after scan conversion with the PC monitor.

In the future we will turn our focus towards the application of real time strain imaging in other areas of ultrasound diagnosis such as the female breast, IVUS, imaging of the thyroid, imaging of liver, kidney and other abdominal organs.

ACKNOWLEDGEMENTS

REFERENCES

[1] J. Ophir, I. Céspedes, H. Ponnekanti, Y. Yazdi, X. Li, "Elastography, a quantitative method for imaging the elasticity of biological tissues", Ultrasonic Imaging Vol. 13, pp. 111-134, 1991

[2] A. Pesavento, C. Perrey, M. Krueger, H. Ermert, "A time efficient and accurate strain estimation concept for ultrasonic elastography using iterative phase zero estimation", IEEE

Trans. on Ultrason., Ferroelect. & Freq. Control, Vol. 46, Part 5 pp. 1057-1067, 1999

[3] I. Céspedes , Y. Huang, J. Ophir and S. Spratt "Methods for the estimation of subsample time delays of digitized echo signals", Ultrasonic Imaging, vol. 17, p. 142-171, 1995

[4] J. P. Reilly, Matrix Computations for Signal Processing, EE731 Lecture Notes, McMaster University, 1998

[5] B. Friedlander, "On the Cramer-Rao bound for time delay and doppler estimation," IEEE Trans. Inform. Theory, vol. 30, no. 3, pp. 575-580, 1984.

[6] A. Pesavento, A. Lorenz, S. Siebers, H. Ermert, "New real-time strain imaging concepts using diagnostic ultrasound", Phys. Med. Biol, vol. 45, pp 1423-1435, 2000

[7] A. Pesavento, A. Lorenz, H. Ermert, "A system for realtime elastography." IEEE Trans. on Ultrason., Ferroelect. & Freq. Contr., vol. 35, Part. 11, pp. 941-942, 1999

[8] A. Lorenz, H.-J. Sommerfeld, M. Garcia-Schürmann, S. Philippou, T. Senge, H. Ermert, "A new system for the acquisition of ultrasonic multicompression strain images of the human prostate in vivo", IEEE Trans. on Ultrason., Ferroelect. & Freq. Contr. Vol. 46, Part 5, pp. 1147-1154, 1999

[9] H. Schmid, H., J. E. Altwein, P. Faul, M. Wirth, "Screening und Früherkennung des Prostatakarzinoms", Deutsches Ärzteblatt, vol. 96, Part 12, p. 772-777, 1999

[10] P. Chaturvedi P, M. F. Insan, and T. J. Hall "2-D Companding for noise reduction in strain imaging" IEEE Trans. Ultrason., Ferroelect., Freq. Contr., vol. 45, pp. 179-191

[11] A. Lorenz A, H. Sommerfeld H, M. Garcia-Schürmann, S. Philippou S, T. Senge, H. E. Philippou, T. Senge, and H. Ermert „Diagnosis of prostate carcinoma using multicompression strain imaging: data acquisition and first in vivo results" Proc. of the 1998 IEEE Ultrasonic Symposium pp 1761-1764, 1998